



Seasonal changes of the South American monsoon system during the Mid-Holocene in the CMIP5 simulations

M. H. Shimizu¹ · G. Sampaio¹ · I. M. Venancio¹ · J. Maksic¹

Received: 6 June 2019 / Accepted: 14 January 2020 / Published online: 23 January 2020
© Springer-Verlag GmbH Germany, part of Springer Nature 2020

Abstract

The South American Monsoon System (SAMS) is a major climatic feature of South America, and its domain extends from Amazon to La Plata basin. The SAMS region is vulnerable to variations of climate and precipitation patterns, which could impact economic activities and lead to potential societal consequences. In the face of a warming future scenario, the importance of the study of the past climate with numerical simulations is to evaluate the climate models and to assure the reliability of future projections. Here we investigate the Mid-Holocene SAMS, evaluating changes in strength, life cycle and associated dynamical mechanisms in ten Earth System Models simulations. Our results show that the SAMS was weaker in the Mid-Holocene than in the pre-industrial climate in December–January–February (DJF), but stronger in September–October–November (SON). This is probably a consequence of insolation variations in the Mid-Holocene, which contributed to changes in the moisture flux from the Atlantic Ocean to the continent, the strength of the upper-level atmospheric circulation, and the amount of precipitation over the SAMS region. Moreover, we suggest that the life cycle of the SAMS was altered during the Mid-Holocene, with an earlier onset and demise. Our results also indicate that Mid-Holocene SAMS changes are connected to precipitation variations near Northeast Brazil, in a dipole configuration of precipitation between western Amazon and Northeast Brazil, due to the influence of the Walker cell. Finally, this study highlights a need for improvement of the numerical models to better simulate the amount of precipitation over South America and the upper-level circulation over western Amazon in SON, which are crucial factors for a more realistic representation of the SAMS.

Keywords South American monsoon system · Mid-Holocene · CMIP5 · Climate change

1 Introduction

Monsoon systems are the dominant mode of climate variability over the tropics, impacting about 70% of the world's population. Most of these populations live in developing countries and are dependent on the variability of the monsoon, such as onset and demise dates, as well as total amount and intensity of precipitation, for agricultural activities (Mohtadi et al. 2016). The South American Monsoon System (SAMS) is the most significant climatic feature of South America, responsible for the largest amount of the annual precipitation over most of the continent extending

from the Amazon River basin to the south of La Plata basin (Gan et al. 2004; Marengo et al. 2012).

The life cycle of the SAMS starts in the austral spring (September to November, SON), with the development of the deep convection over northwestern Amazon, associated to an upper-level anticyclonic circulation, which spreads progressively to southeastern Brazil by the middle of November (Kousky 1988; Gan et al. 2004). The mature phase of the SAMS occurs during the austral summer (December to February, DJF), with the establishment of an upper-level anticyclone over Bolivia, known as the Bolivian High (BH), and a trough over the Atlantic Ocean, known as the Northeast Low (NL; Virji 1981; Chen et al. 1999), and the presence of the South Atlantic Convergence Zone (SACZ), which is a cloud band, in a northwest-southeast orientation, associated with low-level moisture convergence and significant amounts of precipitation (Kodama 1992, 1993; Carvalho et al. 2002).

The variability of the SAMS can be influenced by remote ocean–atmosphere interactions. The tropical Atlantic Ocean

✉ M. H. Shimizu
marilia.shimizu@gmail.com

¹ Center for Weather Forecasting and Climate Studies, National Institute for Space Research, Cachoeira Paulista, São Paulo, Brazil

influences the interannual rainfall variability, especially over the Amazon River basin (Yoon and Zeng 2010; Marengo et al. 2011), through the modulation of the north–south divergent circulation and the Intertropical Convergence Zone (ITCZ) movement following warm Sea Surface Temperature (SST). Over the tropical Pacific Ocean, the El Niño Southern Oscillation (ENSO) is the most important phenomenon influencing interannual precipitation and temperature variability over the South American continent, explaining about two-thirds of the interannual variance of precipitation and temperature (Garreaud et al. 2009).

On geological time scales, SAMS's precipitation variability is mainly influenced by two factors: (1) variations in orbital parameters, and (2) the meridional gradient of the Atlantic SST (Baker and Fritz 2015). Variations in greenhouse gas concentrations and glacial boundary conditions are also considered as an additional driver of the climate (Cook and Vizy 2006; Kanner et al. 2012). Orbital-scale changes cause variations in insolation that ultimately influence the intensity of the SAMS and the position of the ITCZ (Seltzer et al. 2000; Haug et al. 2001; Baker et al. 2001a; Cruz et al. 2005). In addition, the meridional gradient of the Atlantic SSTs causes an impact on precipitation over the northern part of the SAMS through the modulation of the ITCZ latitudinal positioning (Nobre and Shukla 1996) and changes in the meridional circulation (Coelho et al. 2012). ENSO variability is insufficient to explain most of the variations of the SAMS precipitation observed in the Holocene paleoclimatic records (Baker and Fritz 2015) since there is no evidence that ENSO might have been more frequent in the late Holocene (Cobb et al. 2013).

In the Mid-Holocene (6000 years ago, 6 ka), the SAMS intensity was weaker than in the present, with reduction in precipitation, according to speleothems records from the Peruvian Andes (Cheng et al. 2013; Kanner et al. 2013) and southeastern Brazil (Cruz et al. 2005), and ice cores from Peru (Thompson et al. 1995) and Bolivia (Ramirez et al. 2003). A weaker SAMS during the Mid-Holocene was also simulated by climate models (Silva Dias et al., 2009; Prado et al. 2013; Maksic et al. 2019). On the other hand, there was an increase in precipitation during the Mid-Holocene in Northeast Brazil and eastern Amazon, as indicated by proxies in speleothems (Cruz et al. 2009; Cheng et al. 2013; Wang et al. 2017) and climate models (Prado et al. 2013; Maksic et al. 2019). The mechanisms associated with the SAMS weakening and the precipitation dipole between western Amazon and Northeast Brazil will be investigated in this study.

Model simulations of past climates are a powerful mean to help in understanding the mechanisms of the past variability of the SAMS precipitation. The results from climate models could support the interpretation of paleoclimatic records from South America, which have a limitation in providing

information about dynamical variables and atmospheric circulation. In this context, Coupled Model Intercomparison Project phase five (CMIP5; Taylor et al. 2012) designed a new series of coordinated experiments to evaluate the ability of climate models to simulate past scenarios and assess the sensibility of the climate to changes in atmospheric composition and biosphere. These experiments include simulations of the Pre-Industrial period (before 1850), Historical period (1850–2005) and the Mid-Holocene (6 ka). In this context, this study aims to investigate the changes in precipitation and atmospheric circulation linked to the SAMS during the Mid-Holocene using the results of the CMIP5 models. Data and methodology used in this study are presented in Sect. 2. Climate simulations are briefly described in Sect. 3, while the analysis and discussions of these simulations and the mechanisms associated with the Mid-Holocene climate changes are in Sect. 4. Finally, Sect. 5 presents the main conclusions.

2 Data and methodology

2.1 Data

In this section, we present a description of the observed data used in the model validation, the CMIP5 models selected for the analysis, and the numerical experiments studied here.

For the observed data, as South America presents an irregular spatial distribution of precipitation from station data, we choose to use monthly precipitation data from the Climate Prediction Center (CPC) Merged Analysis Precipitation (CMAP, Xie and Arkin 1997), which merges observation from rain gauges with precipitation estimates from satellites (starting from 1979). Monthly data of 1.5 m air temperature and wind are from ERA-Interim reanalysis of the European Centre for Medium-Range Weather Forecast (ECMWF, Dee et al. 2011). The horizontal resolution of CMAP and ERA-Interim are 2.5° and 1.5°, respectively, and the period analyzed was the same for both datasets, from 1979 to 2004. Figure 1 shows precipitation and upper-level circulation for SON and DJF derived from these datasets, and illustrate the main features of the SAMS, such as the SACZ, ITCZ, BH, and NL.

The model data for the present climate and Mid-Holocene were obtained from the British Atmospheric Data Centre (BADC). We analyzed the results of ten CMIP5 Earth system models, whose main characteristics are shown in Table 1, for the experiments *Pre-Industrial*, *Historical* and *Mid-Holocene*. The parameters for these climate simulations were defined by the protocol established by CMIP5 (Taylor et al. 2012). A brief description of these CMIP5 experiments is given below, with the main forcings for each period.

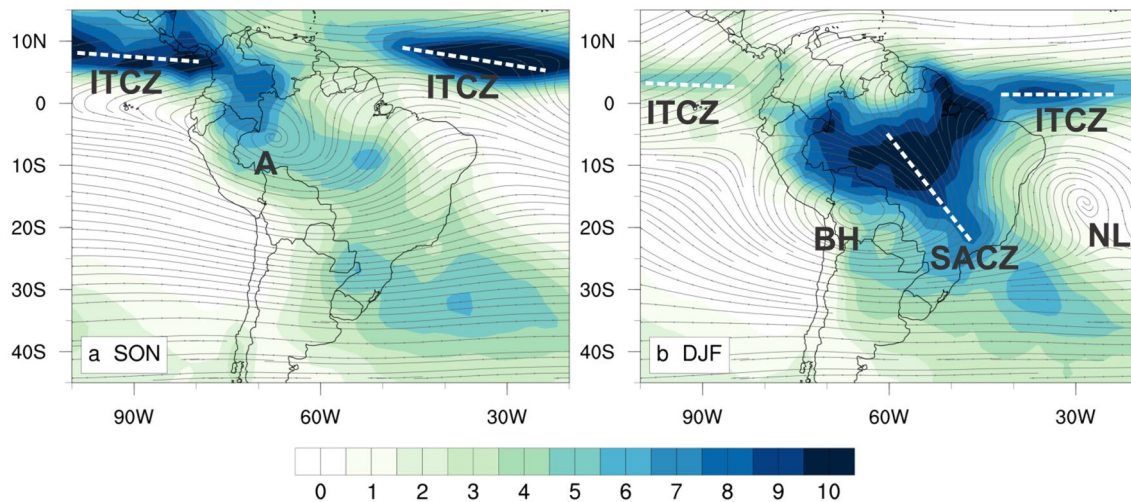


Fig. 1 Precipitation (mm/day) and 200 hPa circulation from 1979–2004 CMAP and ERA-Interim reanalysis data, respectively, for (a) SON and (b) DJF. The main atmospheric features illustrated are the

ITCZ, SACZ, Bolivian High (BH), Northeast Low (NL), and anticyclonic circulation (A)

Table 1 CMIP5 Earth system models analyzed in this study, with the atmospheric resolution (lat x lon grid; number of vertical levels) and references

Model	Institute	Atmospheric grid	References
BCC-CSM1.1	Beijing climate center (BCC, China)	~2.8° × 2.8°; 26	Xin et al. (2013)
CCSM4	National center for atmospheric research (NCAR, USA)	1.25° × 0.9°; 27	Gent et al. (2011), Brady et al. (2013)
CNRM-CM5	Centre national de recherches meteorologiques—Centre Europeen de recherche et formation avancees en calcul scientifique (CNRM-CER-FACS, France)	~1.4° × 1.4°; 31	Voldoire et al. (2013)
CSIRO-Mk3-6-0	Commonwealth scientific and industrial research organization (CSIRO, Australia)	~1.875° × 1.875°; 18	Rotstayn et al. 2012
GISS-E2-R	National Aeronautics and Space Administration (NASA, USA)	2° × 2.5°; 40	Schmidt et al. 2014
HadGEM2-ES	UK met office hadley center	1.25° × 1.875°; 38	Collins et al. (2011), Jones et al. (2011)
IPSL-CM5A-LR	Institute Pierre-Simon Laplace (IPSL, France)	1.9° × 3.75°; 39	Dufresne et al. (2013), Braconnot and Kageyama (2015)
MIROC-ESM	University of Tokio, national institute for environmental studies, Japan agency for marine-earth science and technology (MIROC, Japan)	2.8° × 2.8°; 80	Watanabe et al. (2011), Sueyoshi et al. (2013)
MPI-ESM-P	Max planck institute for meteorology (MPI-M, Germany)	~1.9° × 1.9°; 47	Giorgetta et al. (2013), Bothe et al. (2013)
MRI-CGCM3	Meteorological research institute (MRI, Japan)	~0.9° × 0.9°; 48	Yukimoto et al. (2012)

The *Pre-Industrial* (PI) experiment serves as the baseline, with the values for greenhouse gases, aerosols, ozone, and solar irradiance fixed at the year 1850. The results of this experiment are used as initial conditions for historical and paleoclimatic simulations, and to estimate the unforced variability of the model. The *Historical* experiment covers the period between 1850 and at least 2005, and it aims to evaluate the model performance against the present climate and

observed climate change. External forcings include observed greenhouse gas concentration, solar forcing, volcanic activity, ozone, and aerosols. The *Mid-Holocene* experiment is a climate simulation for 6000 years ago with imposing conditions consistent with the Paleoclimate Modeling Intercomparison Project phase three (PMIP3) specifications (Braconnot et al. 2011, 2012), including Mid-Holocene values for orbital parameters and atmospheric concentrations

of greenhouse gases, which did not change throughout the model integration. The main purpose of this experiment is to compare paleodata with the model response to orbital forcing and greenhouse gas concentrations changes.

2.2 Methodology

The methodology used in this study is divided into two parts: (1) model validation, which consists of the evaluation of the *Historical* simulation against observations, and (2) Mid-Holocene climate changes, focusing on the precipitation changes and the associated dynamical mechanisms. To evaluate the SAMS changes, our analysis shows the seasonal mean plots for SON and DJF, which is the period when the monsoon is active.

The model validation followed a similar methodology from previous climate change studies with CMIP5 models (Cavalcanti and Shimizu 2012; Dike et al. 2015), with the use of data from satellite and reanalysis operating systems for a climatological period of roughly 30 years. Observed and model data were converted to the same spatial resolution, and the multi-model ensemble mean was calculated. Next, we plot Taylor diagrams (Taylor 2001) of precipitation and temperature to make a comparative assessment of the different models and the multi-model ensemble mean. Finally, we made a comparison between observed data and multi-model ensemble mean to evaluate how well the ensemble mean represents temperature, precipitation, and the main characteristics of the South American atmospheric

circulation. The regions where at least 70% of the models agree, with the sign of the difference between observed data and *Historical* simulation, were emphasized.

To assess the mean state of the Mid-Holocene climate, a 30-year multi-model ensemble mean was calculated for both *PI* and *Mid-Holocene* experiments. Insolation, precipitation, and temperature anomalies, i.e. the difference between *Mid-Holocene* and *PI* ensembles mean, were calculated. We represent the confidence level of the model's results by stippling areas where at least 70% of the models agree with the sign of the difference (i.e., positive or negative anomalies). The statistical significance of the anomalies was tested by *t*-Student's test at a confidence level of 95%. The changes in upper-level circulation, moisture flux content, mean vertical velocity profile, and ITCZ position were also plotted. All figures were made with the software NCL from the National Center for Atmospheric Research (NCAR).

3 Climate simulations

3.1 Model evaluation for the present climate

Here we present the results for the model validation against observed data; a more comprehensive analysis of these simulations is made in Sect. 4. Taylor diagrams of precipitation and temperature for the South American domain (45°S–15°N; 100°W–20°W, Fig. 2) show temporal correlations, root mean square errors (RMSEs), and standardized

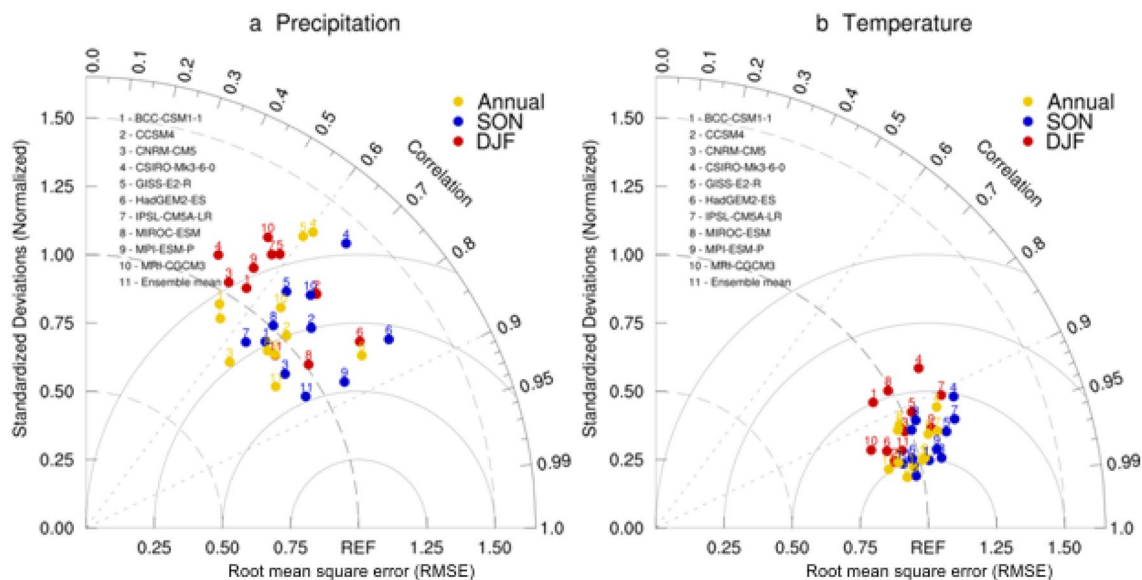


Fig. 2 Taylor Diagram for the Historical simulation (1979–2004) from the CMIP5 models and multi-model ensemble mean in comparison with observations for the annual mean (yellow), DJF (red) and SON (blue) of (a) CMAP precipitation (mm/day), and (b) ERA-

Interim 1.5 m temperature (°C). Root mean square error (RMSE) is represented in the horizontal axis, standardized deviations in the vertical axis, and correlation in the radial axis

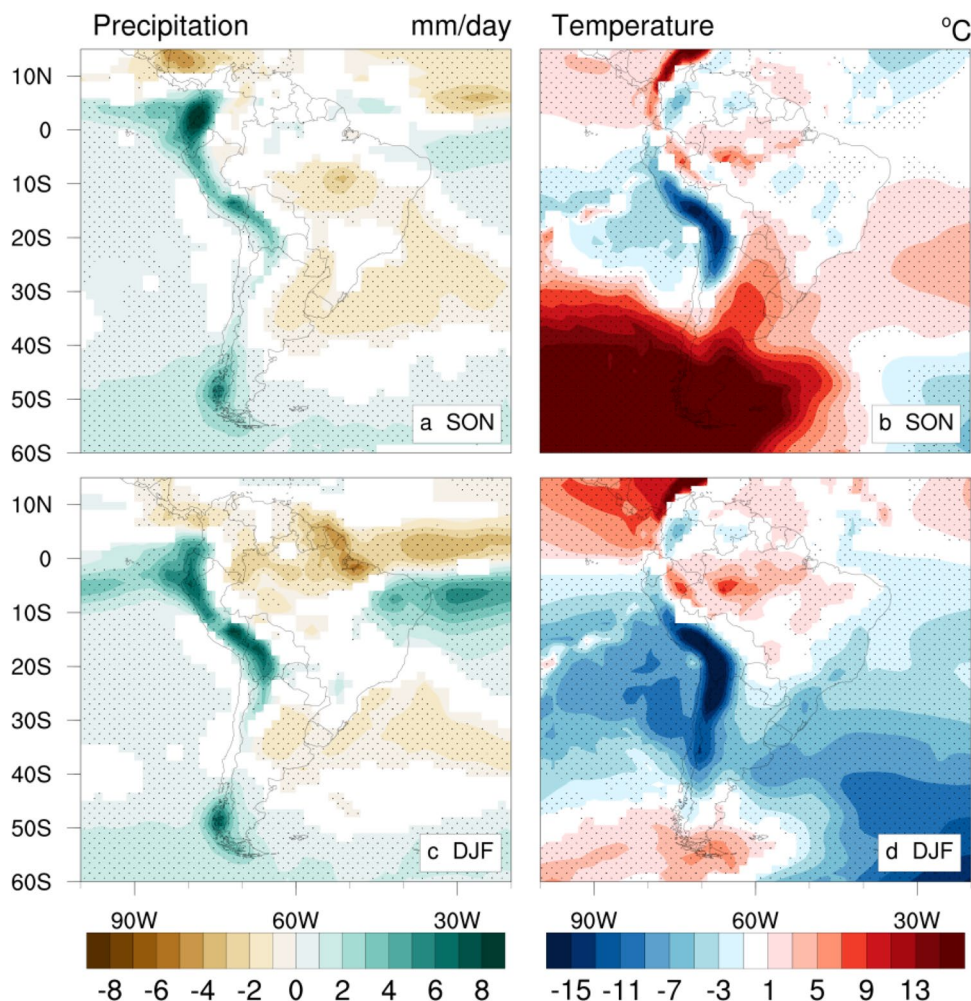
deviations of CMIP5 models and ensemble mean. For the precipitation (Fig. 2a), the models show a dispersion in the values, with some of them with RMSEs larger than 1.25 (e.g. CSIRO-Mk3-6-0 and HadGEM2-ES in SON) and/or correlation lower than 0.6 (e.g. CSIRO-Mk3-6-0 and CNRM-CM5 in DJF). However, the accuracy of the models also depends on the period under analysis, which means that, for example, some models have higher skill in DJF than in SON. Meanwhile, the multi-model ensemble mean (number 11) showed a relatively good agreement with the observations, with low (around 1.0) standard deviation and a correlation between 0.8 and 0.9. Temperature diagram (Fig. 2b) exhibited lower dispersion between the models, with low standard deviation (around 1.0), and a correlation above 0.9 for most of the models, and for the multi-model ensemble mean.

In SON (Fig. 3a), the comparison between observed and *Historical* ensemble mean precipitation showed a small negative bias (< 3 mm/day) over central and southern South America, besides an overestimation over the Andes; these differences are found in at least 70% of the models. In DJF (Fig. 3c), there are large differences

(4–6 mm/day) over the tropical Atlantic Ocean and positive bias (> 8 mm/day) over the Andes Cordillera. All these differences are noted in at least 70% of the models. The differences between the observed data and *Historical* ensemble mean of temperature (Fig. 3b, d) for both DJF and SON show small positive bias (< 3 °C) over the Amazon region, but large cold bias over the Andes Cordillera (> 15 °C). Over southern South America, there is a warm (cold) bias in SON (DJF).

Figure 4 shows the streamlines at 200 hPa upper-level circulation observed and simulated by the *Historical* ensemble mean. In SON, the ensemble mean was not able to reproduce the anticyclone over western Amazon seen in the reanalysis data. In DJF, the BH was reasonably well represented, in terms of wind intensity, by the ensemble mean, but the NL simulated was weaker.

Fig. 3 a, c Differences between *Historical* ensemble mean and CMAP precipitation (mm/day) for SON and DJF. b, d Differences between *Historical* ensemble mean and ERA-Interim 1.5 m temperature (°C) for SON and DJF. Stippling represents areas where at least 70% of the models agree with the sign of the difference. Only significant anomalies at 95% confidence level according to Student's *t* test were plotted



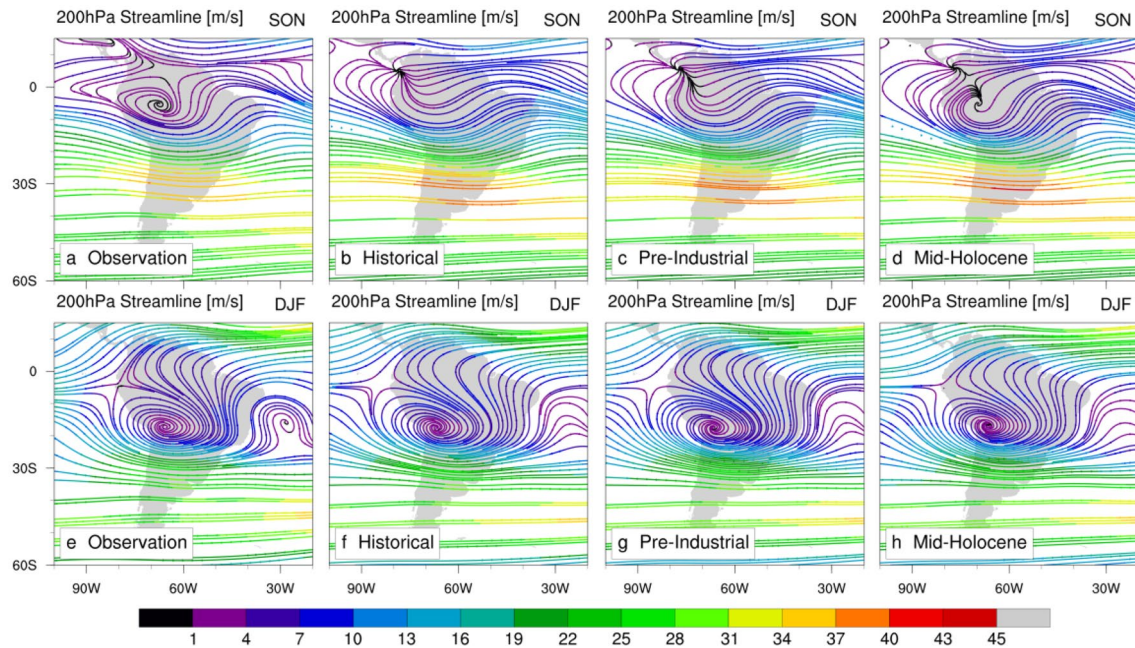


Fig. 4 Streamlines (m/s) at 200 hPa for SON and DJF from (a, e) Observation, (b, f) Historical Ensemble Mean, (c, g) Pre-Industrial Ensemble Mean, (d, h) Mid-Holocene Ensemble Mean

3.2 Mid-Holocene climate simulation

In this section, we present the results of the model's response to Mid-Holocene changes in orbital parameters and greenhouse gas concentration. The analysis and discussions of the Mid-Holocene simulation are made in Sect. 4.

The Mid-Holocene climate is a response to the variations of the insolation, SST and CO_2 concentration. Southern Hemisphere insolation in the Mid-Holocene, defined by the orbital parameters (Berger 1978), was lower (higher) than PI in DJF (SON). These insolation variations are related to an increase of the surface downwelling shortwave radiation flux (Fig. 5a) in SON ($+13.65 \text{ W/m}^2$), and a decrease in DJF (-9.6 W/m^2). SSTs were colder in the Mid-Holocene than the PI conditions, over the tropical oceans (Fig. 5b). Finally, CO_2 concentration for the *Mid-Holocene* experiments was the same as in the PI period, fixed in 280 ppm (Jones et al. 2011).

Figure 6a–d shows the mean precipitation from both Pre-Industrial and Mid-Holocene ensemble means. From these figures, it is possible to observe differences in the amount of precipitation associated with SACZ and Atlantic ITCZ, but not in their mean position. In SON, wet and hot anomalies (Fig. 6e, f) are observed over most of South America, while dry conditions are observed over extratropical South America; there is an agreement of at least 70% of the models in both cases. Changes in precipitation and temperature over Northeast Brazil are not a consensus for at least 70% of the models, but the ensemble mean indicates dry anomalies. In

the Tropical Atlantic, the precipitation was lower than in the PI period, with an agreement of at least 70% of the models.

In DJF, the precipitation over most of South America decreased in the Mid-Holocene (Fig. 6g), with an agreement of at least 70% of the models. In the Northeast Brazil coast and Tropical Atlantic Ocean, there was an increase of precipitation, with also an agreement of at least 70% of the models. The wetter anomalies in the Atlantic ITCZ it is not related to a southward shift in its mean position, but to an increase in the intensity of the precipitation and width of the ITCZ, as evidenced by Fig. 6c, d. Cold anomalies were simulated over South America in DJF (Fig. 6h).

Upper-level anticyclone over Bolivia in SON was configured during the Mid-Holocene (Fig. 4d), which suggests a stronger circulation since this feature was not seen in the *PI* simulation (Fig. 4c). In DJF, the magnitude and position of the BH remained nearly the same as in the PI (Fig. 4g, h).

The vertical profiles of the meridional mean anomalies (12°N – 12°S) of omega (Fig. 7) show a dipole of subsidence/ascendance between the Amazon basin ($\sim 75^\circ$ – 65°W) and Northeast Brazil ($\sim 45^\circ$ – 35°W). There was an increase of ascendance (subsidence) over the Amazon basin (Northeast Brazil) in SON (DJF).

Vertically integrated moisture flux anomalies (Fig. 8a, b) in SON reveal an increase of moisture flux brought from the South Atlantic Ocean by the easterlies (Fig. 8c) into the SAMS region, which is consistent with the wetter conditions in the Mid-Holocene. In DJF (Fig. 8b), a decrease in the moisture flux from tropical North Atlantic and Amazon

Fig. 5 **a** Mean annual cycle of the surface downwelling shortwave radiation flux (W/m^2) for the pre-industrial (0 ka, black line) and Mid-Holocene ensemble means (6 ka, red line), and differences between Mid-Holocene and pre-industrial (6–0 ka, blue line). **b** Differences between Mid-Holocene and Pre-Industrial ensembles mean of annual sea surface temperature ($^{\circ}C$). Dashed areas represent where at least 70% of the models agree with the sign of the difference. Only significant anomalies at 95% confidence level by the Student's *t*-test were plotted

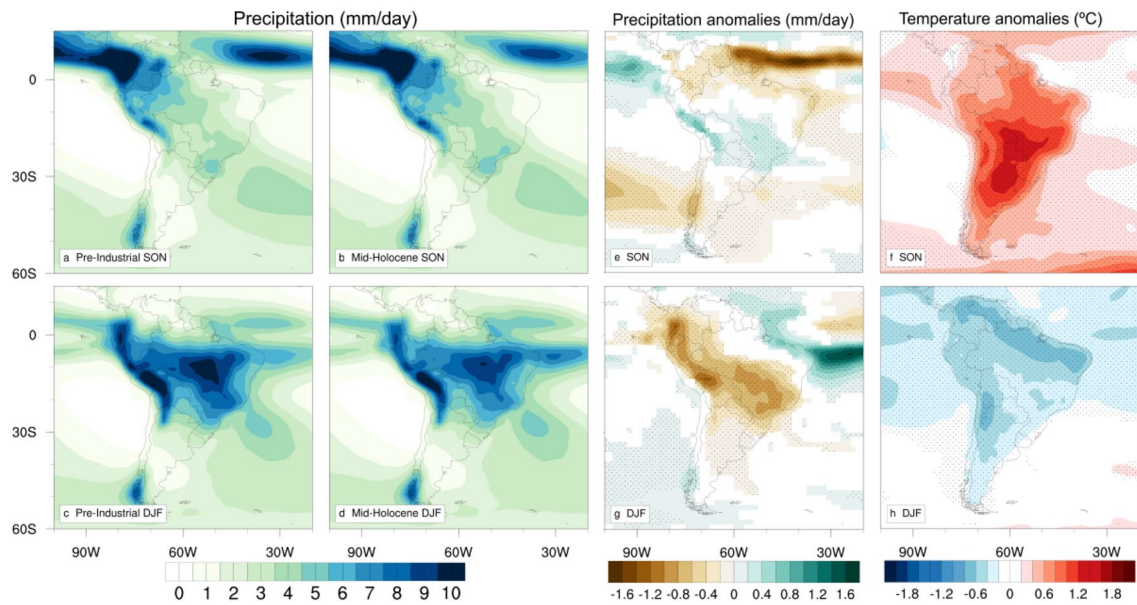
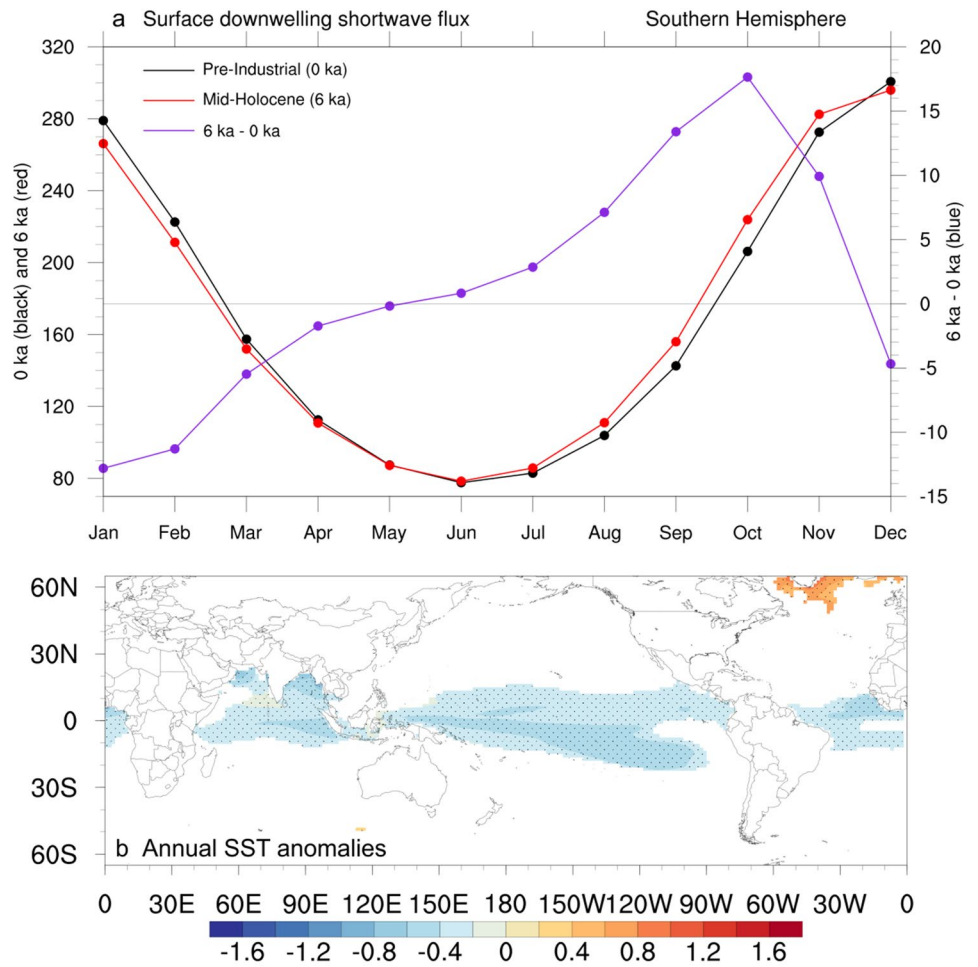


Fig. 6 **a–d** Mean precipitation (mm/day) from **(a, c)** Pre-Industrial Ensemble Mean and **(b, d)** Mid-Holocene Ensemble Mean for SON and DJF. **e–h** Differences between Mid-Holocene and Pre-Industrial ensembles mean of SON and DJF **(e, g)** precipitation (mm/day), and

(f, h) temperature ($^{\circ}C$). Stippling represents areas where at least 70% of the models agree with the sign of the difference. Only significant anomalies at 95% confidence level according to Student's *t* test were plotted

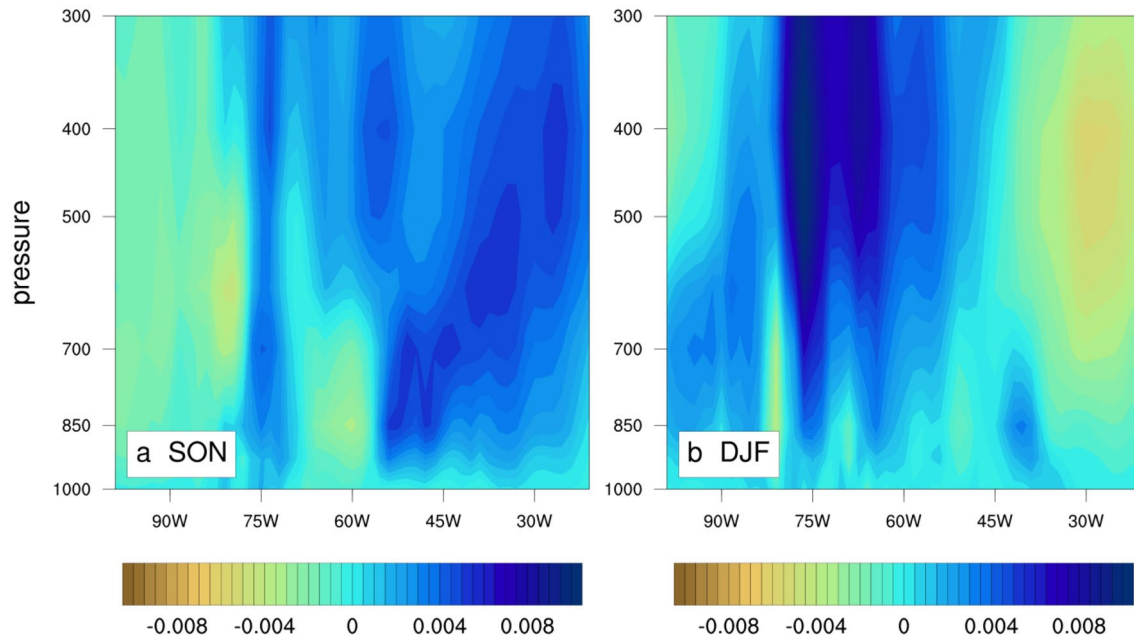


Fig. 7 Vertical profile of the mean meridional (12°N – 12°S) differences between Mid-Holocene and Pre-Industrial ensembles mean of the vertical velocity (ω , Pa/s) in (a) SON and (b) DJF

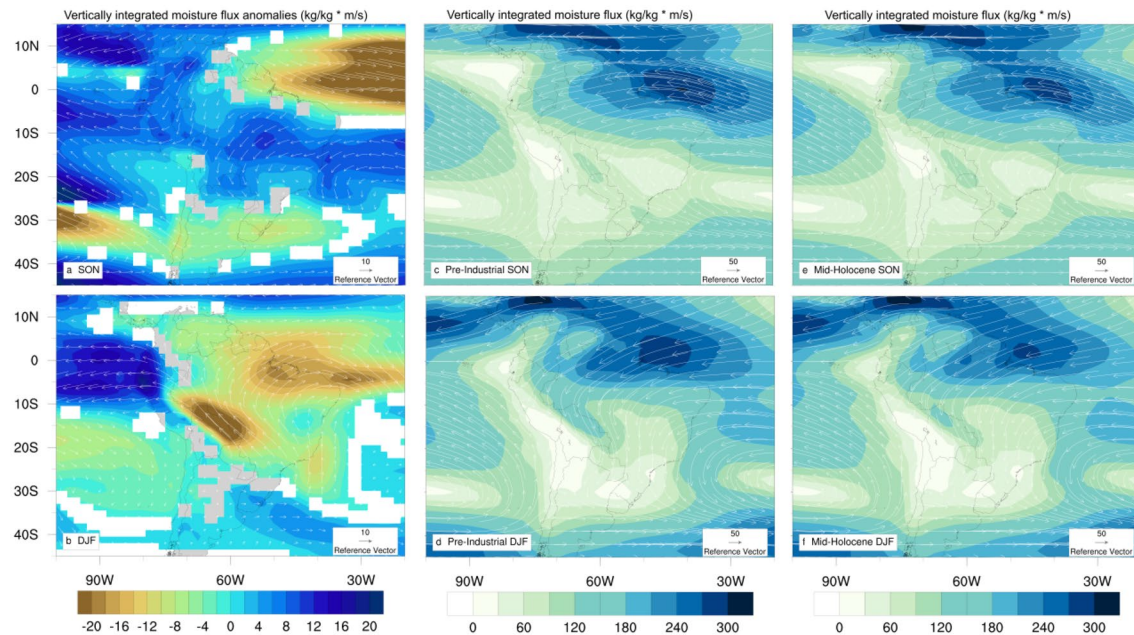


Fig. 8 a–b Differences between Mid-Holocene and Pre-Industrial ensembles mean of vertically integrated moisture flux ($\text{kg}/\text{kg} \cdot \text{m}/\text{s}$) for SON and DJF. Only significant anomalies at 95% confidence level

according to Student's t test were plotted. c–f Vertically integrated moisture flux ($\text{kg}/\text{kg} \cdot \text{m}/\text{s}$) from (c–d) Pre-Industrial and (e–f) Mid-Holocene ensemble means for SON and DJF

(Fig. 8d) is associated with the drier anomalies over the SAMS region. The direction of the moisture source didn't change in the Mid-Holocene (Fig. 8e, f), only the intensity of the moisture flux.

4 Discussions

In this section, we present the analysis and discussions of the model evaluation (Sect. 4.1), as well as the dynamical mechanisms associated to the Mid-Holocene seasonal precipitation changes (Sect. 4.2).

4.1 Model evaluation

4.1.1 Precipitation simulation

The evaluation of the *Historical* simulations against observations (Figs. 2, 3) showed that the main features of the SAMS, such as the northwest-southeast oriented band of precipitation related to the SACZ and the Atlantic Ocean maximum of precipitation associated to the ITCZ, are represented by the ensemble mean. However, there are some discrepancies between observed and simulated precipitation. The models underestimate the precipitation in SON over the SAMS region (Fig. 3) and overestimate the precipitation near the Northeast Brazil coast in DJF. Also, the models simulated a double ITCZ in the Atlantic Ocean, and the maximum precipitation associated with the Atlantic ITCZ is located more to the south than the observed position during both SON and DJF. The deficiency of models to correctly simulate the precipitation over South America was already seen in earlier versions of these models from the CMIP3 experiments (Boullanger et al. 2006; Vera and Silvestri 2009; Seth et al. 2010), with overestimation of precipitation over the Andes and underestimation over Amazon and the Atlantic ITCZ.

Despite the recent efforts to improve climate models and to reduce precipitation biases, some CMIP5 models are still not able to reproduce the rainfall over Amazon, due to the underestimation of the large-scale precipitation, and biases of surface latent and sensible fluxes (Yin et al. 2013). Moreover, the dry biases could be caused by the simulation of stronger ITCZ over the tropical Atlantic and eastern Pacific Oceans, which results in strong moisture divergence and low cloud amounts over Amazon (Yin et al. 2013). Besides, most of the models simulated a double ITCZ over the Atlantic Ocean in DJF (Adam et al. 2018, and references therein), which is not realistic. Double ITCZ simulation is a bias that persists from CMIP3 to CMIP5 (Zhang et al. 2015; Jones and Carvalho 2013), and the main causes include poor representation of ocean–atmosphere feedbacks, SST biases, and extratropical cloud biases (Li and Xie 2014).

Over southern South America, the dry bias in SON could be related to an incorrect simulation of the amount of precipitation resulting from the onset of the SAMS and frontal systems incursions. However, these dry biases are not seen in an earlier analysis with seven CMIP3 models and University of Delaware precipitation data (Vera et al. 2006), meaning that the model evaluation is also dependent on the dataset used to represent the “observed precipitation”.

4.1.2 Upper-level atmospheric circulation simulation

One feature that is not represented by the CMIP5 models is the upper-level anticyclonic circulation over Bolivia in SON (Fig. 4b). This circulation is not seen in September, but is configured in October and November in the reanalysis data

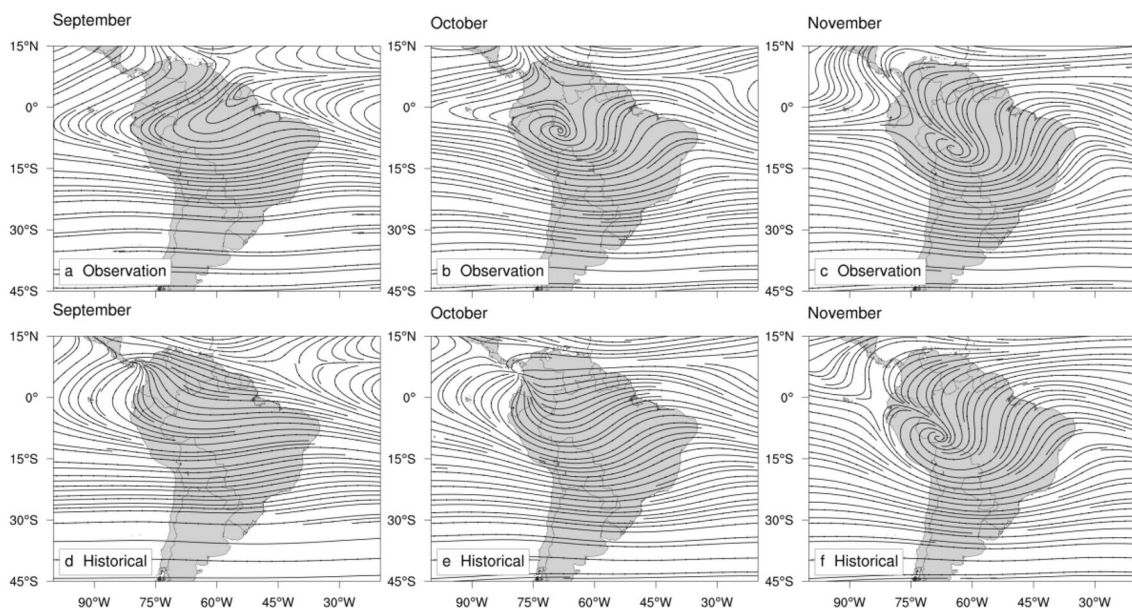


Fig. 9 Streamlines at 200 hPa (m/s) in September, October, and November for (a, b, c) observation, and (d, e, f) Historical ensemble mean

(Fig. 9a–c). However, the *Historical* ensemble mean only shows this anticyclonic circulation in November (Fig. 9d–f). That is the reason why the high-pressure circulation is not seen in the seasonal mean (SON). The late development of the anticyclonic circulation by the models can be related to the parameterization of convection and radiation processes, once the anticyclone formation is a dynamical response to the high troposphere heating due to cumulus convection over Amazon basin (Lenters and Cook 1997). The misrepresentation of this upper-level anticyclone is also related to the dry bias in SON in the SAMS region.

Despite the models don't represent the same pattern of precipitation, atmospheric circulation, and Atlantic ITCZ, our results can be useful to assess the climate response to orbital forcing and greenhouse gases emissions and to understand the dynamical mechanisms that caused the changes in the precipitating systems and atmospheric circulation during the Mid-Holocene. The confidence level of the Mid-Holocene changes is restricted to where at least 70% of the models agree with the sign of the difference, regardless of the intensity of these changes.

4.2 Mid-Holocene simulations

Mid-Holocene climate simulations showed mainly the climate system response to changes in the mean seasonal cycle of insolation and SSTs. Numerical experiments on the relative importance of insolation and SST showed that insolation is the dominant forcing to land temperature and north–south displacement of the continental convection, while SST is responsible for the determination of the ITCZ location (Biasutti et al. 2003). In this section, we evaluate separately these two influencing climate factors to the SAMS strength.

4.2.1 Insolation variations

Here, we explore the seasonal changes of the insolation, driven by orbital parameters variations, and how it influences the precipitation and circulation changes. Orbital parameters for the Mid-Holocene lead to an increase of the insolation in SON and decrease in DJF over the Southern Hemisphere, affecting the surface downwelling shortwave radiation flux (Fig. 5a). So, the variations of the energy budget, i.e. a surplus (deficit) of surface shortwave radiation in SON (DJF), caused a surface warming (cooling) over most of South America (Fig. 6f, h), which is primarily responsible for the precipitation and circulation changes.

The insolation influence on SAMS precipitation in DJF found in our results is consistent with earlier studies. For example, Liu et al. (2003) concluded that the summer precipitation over South America was reduced mainly due to the reduced insolation, and our results are in agreement with these results. Other climate simulations for the

Mid-Holocene (Biasutti et al. 2003; Prado et al. 2013; Liu and Battisti 2015; Braconnot et al. 2007b) also showed, as our results (Fig. 6g), that the decrease of summer precipitation over SAMS region is caused by the lower insolation. However, our results went further than the previous one because we explored the dynamical mechanisms related to these rainfall changes.

For a comparison between paleoclimate proxies (see location and references in Fig. 10) and models, we analyze the ensemble mean for the annual precipitation and precipitation minus evaporation (P–E) anomalies (Fig. 10). The results show reduction of precipitation over the SAMS and are consistent with paleoclimate proxies in lake sediments and speleothems (Seltzer et al. 2000; Baker et al. 2001b; Cruz et al. 2009; Strikis et al., 2011; Novello et al. 2017), which show evidence of the weakening of the SAMS and reduction of precipitation due to the lower insolation. However, other proxies in the SAMS region (e.g., Kanner et al. 2013; Wang et al. 2017) show wetter conditions, which is in disagreement with the model's results. This could be related to a misrepresentation of the local sources of moisture, such as water recycling over the Amazon Basin (Cheng et al. 2013; Wang et al. 2017).

Regarding the influence of the insolation variations on the SAMS precipitation, an important contribution of our study is the precipitation changes in SON, which was not entirely explored by earlier studies.

4.2.2 SST variations

In this section, we discuss the SST influence on the SAMS in the Mid-Holocene. Our results with the CMIP5 ensemble mean show an almost uniform cooling along the tropical oceans (Fig. 5b), which agree with earlier modeling studies from PMIP2 and PMIP3 (Braconnot et al. 2007a; Ann and Choi 2014). Over the eastern Pacific, our results are consistent with Mid-Holocene SST reconstructions derived from a synthesis of proxies (Carré et al., 2012) that suggests persistent colder eastern Pacific SSTs.

The larger impact of tropical Pacific SST changes on precipitation over southern South America during the Mid-Holocene seems to be related to the colder Pacific SSTs. Drier conditions over southern South America in SON and DJF (Fig. 6e, g) could have been induced by teleconnections driven by the permanent colder Tropical Pacific SSTs, in analogy to the present climate effects of La Niña on precipitation over this region, as suggested by Carré et al. (2012).

On the other hand, Atlantic SST changes are associated with the strength of the SACZ, which is weakened by cold anomalies in the Atlantic (De Almeida et al. 2007). This influence can be another factor that contributed to the reduction of the precipitation in DJF over the region of the SACZ and SAMS (Fig. 6g). Also, colder SSTs over the tropical

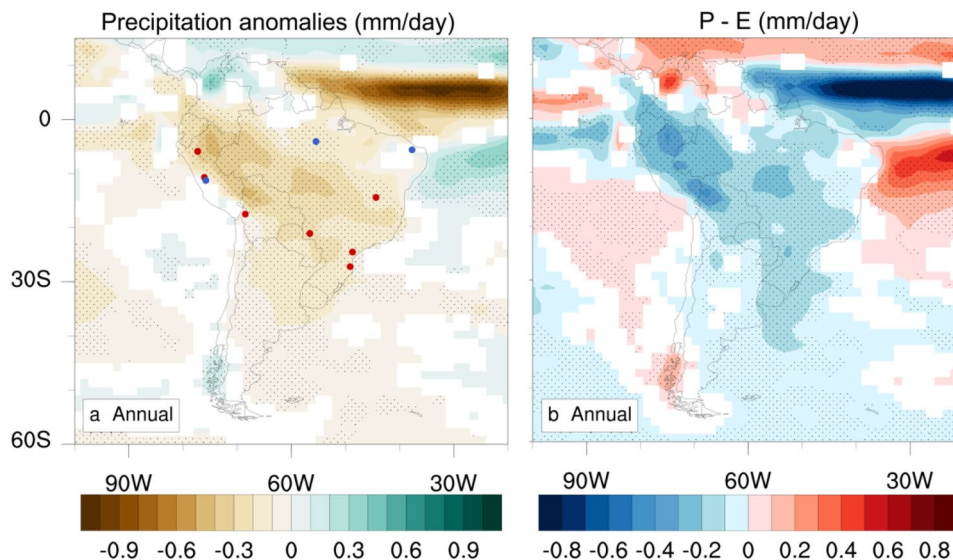


Fig. 10 Differences between Mid-Holocene and Pre-Industrial ensembles mean of annual (a) precipitation (mm/day), and (b) precipitation minus evaporation (P-E, mm/day). Stippling represents areas where at least 70% of the models agree with the sign of the difference. Only significant anomalies at 95% confidence level according to Student’s *t*-test were plotted. The red and blue points indicate the location of the paleoclimate proxies from Jaraguá cave (Novello et al.

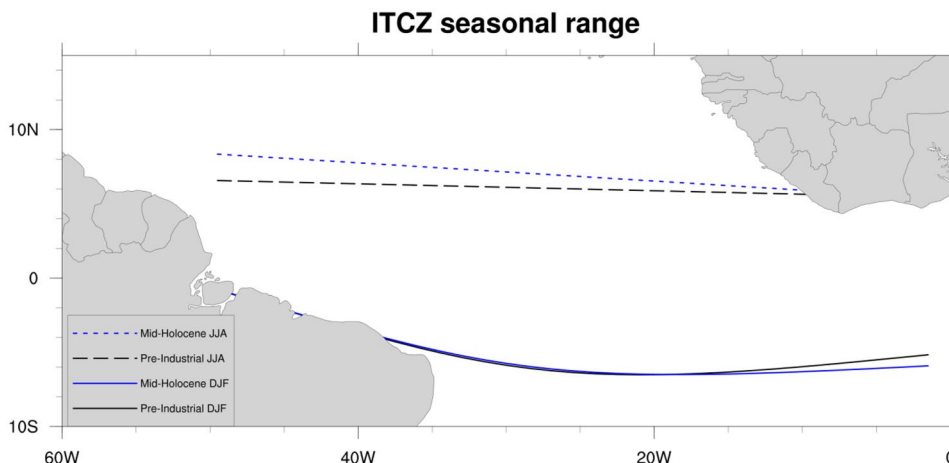
2017), Santana cave (Cruz et al. 2006), Lapa Grande cave (Strikis et al. 2011), Pumacocha lake (Bird et al. 2011), Titicaca lake (Baker et al. 2001b), El Condor cave (Cheng et al. 2013), Rio Grande do Norte caves (Cruz et al. 2009), Huagapo cave (Kanner et al. 2013), Tigre Perdido cave (van Breukelen et al. 2008) and Paraíso cave (Wang et al. 2017). Red (blue) points indicate drier (wetter) conditions

Indian Ocean could be associated to the dry anomalies over central Brazil, in a mechanism similar to the positive phase of the Indian Ocean Mode (Chan et al. 2008).

The impact of the tropical Atlantic SST gradient on precipitation over Northeast Brazil was analyzed indirectly by tracking the ITCZ position. We tested the hypothesis that precipitation changes in the tropical Atlantic Ocean, near the coast of Northeast Brazil, would imply a meridional displacement of the ITCZ position. However, the estimations of the ITCZ position (Fig. 11), using the minimum values of the simulated Outgoing Longwave Radiation (OLR) over the

Atlantic Ocean, showed small (less than 1°) displacements of the ITCZ, which are not sufficient to explain the precipitation changes. These results agree with Liu et al. (2003), which suggest that tropical meridional Atlantic SST gradient influence over Northeast Brazil (Nobre and Shukla 1996) may not be so relevant in geological scales. This small shift of the ITCZ is consistent with previous studies (McGee et al. 2014; Donohoe et al. 2013), which suggest a northward shift of 0.3° related to a weaker South American summer monsoon. Also, the small displacement of the ITCZ showed in Fig. 10 is corroborated by the mean precipitation fields for

Fig. 11 Mean ITCZ position from Mid-Holocene (6 ka) and Pre-Industrial (0 ka) ensembles mean during DJF and JJA derived from the minimum values of outgoing longwave radiation (OLR)



PI and Mid-Holocene (Fig. 6 c, d), which show an increase of precipitation and width of the Atlantic ITCZ, instead of a meridional shift.

4.2.3 SAMS strength and life cycle changes, and dynamical mechanisms

In this section, we discuss the changes in SAMS strength and life cycle in the Mid-Holocene and the dynamical mechanisms associated with these changes.

Our results show an increase in precipitation over central South America in SON (Fig. 6e) when the onset of the SAMS occurs. This increase of precipitation was related to the strong thermal contrast between the warm continent (Fig. 6f), due to the higher insolation (and surface shortwave radiation flux), and the cold ocean (Fig. 5b). This thermal land-sea gradient increased the upper-level anticyclonic circulation over northwestern Amazon (Fig. 4c, d), which contributes to a moisture flux towards central and southern South America (Fig. 8a), and to an increase of precipitation over the central-south regions of the SAMS.

On the other side, northern and northwest Amazon was drier during Mid-Holocene in SON, due to the subsidence associated with the Walker cell (Fig. 7a). Recent studies (Barichivich et al. 2018; Espinoza et al. 2019) have reported that in the last decades Walker cell is influencing precipitation over northern and northwest Amazon in an opposite way. Increasing trends in rainfall since the late 1990s have been associated with the intensification of Walker and Hadley cells. In both cases, the increase of the radiative forcing (higher insolation in the Mid-Holocene and intensification of the greenhouse effect by anthropogenic emissions in the present) has an important role, but other mechanisms must be taken into account for the recent trends, such as the multi-decadal variability (Wang et al. 2018). Few previous studies (Melo and Marengo 2008; Maksic et al. 2019) analyzed the changes in the Mid-Holocene in SON, but the results were contrasting. While Melo and Marengo (2008) showed drier conditions over SAMS in SON and DJF, Maksic et al. (2019) showed wetter conditions in SON. Our results are consistent with the findings of Maksic et al. (2019), although these authors did not explore in detail the changes in circulation and moisture flux.

On the other hand, the precipitation in DJF decreased over most of South America because of the lower insolation and weaker moisture flux from the North Atlantic and Amazon (Fig. 8b). The weakening of the precipitation in DJF along with the enhancement of the precipitation in SON over the SAMS region suggests that the SAMS life cycle changed during the Mid-Holocene. If we compare the precipitation anomalies during SAMS onset (September to November, Fig. 6e) and mature phases (December to February, Fig. 6g), we can hypothesized that the

SAMS life cycle changed in the Mid-Holocene, with a larger (lower) amount of precipitation during the onset (mature) phase.

Hence, our results show that the wetter conditions in SON, and possible anticipation of the onset of the rainy season, are associated with the strengthening of the upper-level anticyclone and increase of moisture flux from the North Atlantic and Amazon.

4.2.4 East–west antiphasing precipitation

In this section, we explore how SAMS changes are connected to variations in Northeast Brazil, which is primarily influenced by the Atlantic ITCZ.

Over Northeast Brazil, the precipitation changes (Fig. 6e, g) are the opposite of what is observed for the SAMS, which means that there was an increase (decrease) of precipitation in DJF (SON). This dipole of precipitation between Amazon and Northeast Brazil is associated with changes in the Walker Cell, as showed by the vertical profile of atmospheric circulation (Fig. 7). Previous modeling studies (Liu et al. 2004; Harrison et al. 2003; Prado et al. 2013; Maksic et al. 2019) indicated that Northeast Brazil was wetter in DJF. However, these studies did not show any evidence for drier conditions in SON.

From the historical records, the dipole pattern between dry Amazon and wet Northeast Brazil is becoming less frequent during the last recent decades (Marengo et al. 2013), while the opposite (wet Amazon/ dry Northeast Brazil) has an increasing trend. This is consistent with the Holocene simulation from Maksic et al. (2019) that indicated a drier trend for Northeast Brazil since 8 ka. Also, this dipole pattern has been observed during extreme events, such as the intense La Niña event in 2012, with floods in Amazon and drought in Northeast Brazil (Marengo et al. 2013). The mechanisms controlling this antiphasing pattern involve local and remote influences. Tropical Pacific SSTs modulated the upward vertical motion and the rainfall in northern South America through Walker cell, while anomalous surface pressure areas over the Atlantic Ocean control the precipitation over Northeast Brazil.

Our analysis is seen to confirm the results presented by Cruz et al. (2009), which suggested a zonally oriented antiphasing of precipitation between Northeast Brazil and the rest of southern tropical South America. Their analysis indicated to humid (arid) conditions over Northeast Brazil during low (high) summer insolation, whereas Amazon showed opposite characteristics. As in our case, the mechanisms responsible for the precipitation changes were the insolation-driven variations in the convective patterns and large-scale circulation.

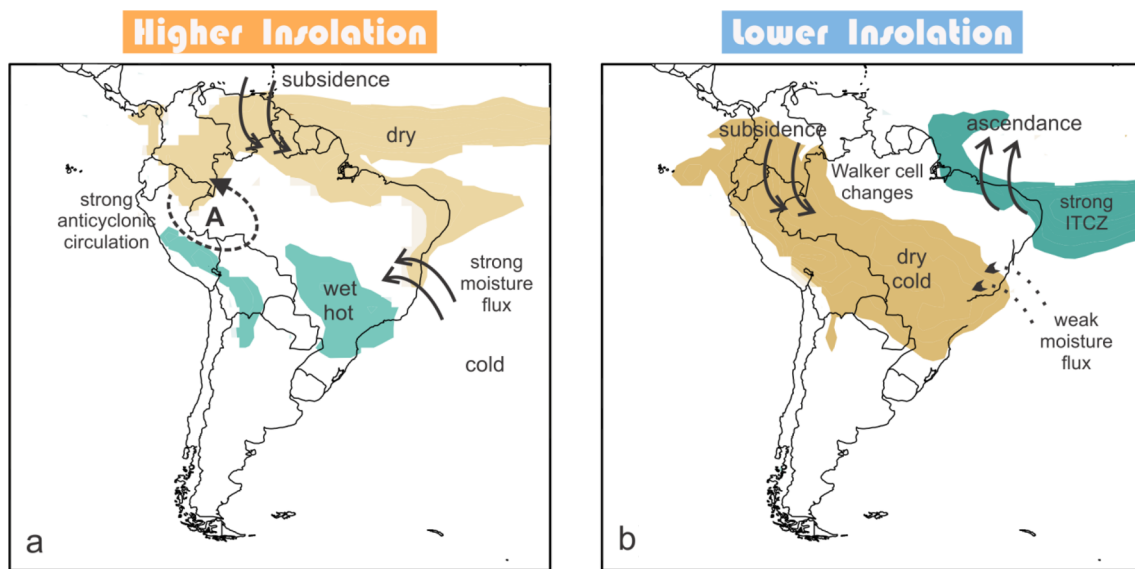


Fig. 12 Schematic diagram illustrating the mechanisms associated with Mid-Holocene climate changes in (a) SON and (b) DJF. In SON, the higher insolation warms the continent, and the strong land-sea thermal gradient enhances the atmospheric circulation and the moisture flux, which leads to an increase of precipitation over central-

south South America. In DJF, the cooling of the surface reduces the moisture flux and precipitation over the SAMS region, while Walker cell changes are connected to increased rainfall over Northeast Brazil and the Atlantic ITCZ

4.3 Summary of the discussions

The main changes in the SAMS during Mid-Holocene and the mechanisms associated are summarized in Fig. 12. In SON, the higher insolation enhanced the thermal gradient between the warm land and the cold ocean. This thermal contrast leads to an intensification of the upper-level anticyclonic circulation and moisture flux, which increased the precipitation over central-south South America. In DJF, the weaker moisture flux, due to the cooling of the surface, reduced the precipitation over the SAMS region. Moreover, there was a dipole pattern of precipitation between the drier western Amazon and the wetter Northeast Brazil (and the Atlantic ITCZ) due to Walker cell changes.

SAMS went through modifications in its strength and life cycle during the Mid-Holocene. Changes in the strength of the SAMS are associated with modifications of the upper-level circulation in response to anomalies in the moisture flux and land-sea temperature gradient. The life cycle of the SAMS was anticipated, with an increase of precipitation in SON and reduction in DJF, as a response to insolation changes.

5 Conclusions

We analyzed the simulations of ten CMIP5 models to investigate the changes in the SAMS precipitation and atmospheric circulation during the Mid-Holocene. The ability of

these models to correctly represent the main features associated with the SAMS was also evaluated against reanalysis data.

Taylor diagrams of temperature and precipitation over South America for the present show a larger dispersion between the models for the precipitation, but a good agreement of the ensemble mean to the observations for both variables. The ensemble mean of the CMIP5 models can capture the main features of the SAMS, such as the SACZ, and the summer upper-level circulation, but there is a deficiency in the simulation of the amount of precipitation and the spring upper-level anticyclone over western Amazon. The incorrect simulation of the rainfall over Amazon is an issue that was not properly treated by the models from CMIP3 to CMIP5, and the underestimation of the large-scale precipitation, biases of surface latent and sensible fluxes, and incorrect simulation of the ITCZ persist. For the austral spring upper-level circulation, most models delay the development of the anticyclone over western Amazon possibly because of the misrepresentation of the convection and radiation processes.

In the Mid-Holocene simulations, the variations of the mean seasonal cycle of insolation lead to changes in the energy budget, which was primarily responsible for the precipitation and circulation changes (Fig. 12). In SON, the surplus of surface shortwave radiation caused warming over the continent. The higher land-sea thermal contrast and stronger atmospheric circulation lead to an increase in precipitation over the SAMS region. In DJF, the cooling of the surface reduces the moisture flux and precipitation over the SAMS

region. Conversely, near the Northeast Brazil coast, the precipitation increased in DJF and decreased in SON. This dipole pattern of precipitation between Northeast Brazil and western Amazon showed by the CMIP5 ensemble mean was also seen in proxies analysis (e.g. Cruz et al. 2009). Modern and proxy records also show a dipole pattern of precipitation between the Andean region and Northeast, and despite our results agree with these records, we did not discuss this in detail because of the large precipitation biases over the Andes.

We also analyzed the dynamical processes involved in the Mid-Holocene changes. The increase (decrease) of precipitation over the SAMS region in SON (DJF) had a contribution of the positives (negatives) moisture flux anomalies towards central and southern South America. The vertical atmospheric circulation profile showed that the dipole pattern between Amazon and Northeast Brazil was associated with the seasonal changes in the convection and the Walker cell circulation. Walker cell changes have also been observed in the last recent decades over northern and northwestern Amazon (Barichivich et al. 2018; Espinoza et al., 2019), but in this case, the effect has been of increase in precipitation over this region.

The impact of SST changes in Northeast of Brazil precipitation was primarily identified through the changes in the ITCZ position. The small southward shift of the ITCZ in DJF is not sufficient to explain the increase of precipitation near the Northeast Brazil coast. Cold SSTs in the South Atlantic could contribute to the weakening of the SAMS in DJF, while the colder Tropical Pacific SSTs could be an explanation to the drier conditions over southern South America in SON and DJF.

The results from the Mid-Holocene ensemble mean in DJF were consistent with the antiphased pattern of precipitation between the drier western Amazon and the wetter Northeast Brazil coast suggested by speleothem records (e.g. Cruz et al. 2009). Because of the low temporal resolution of the proxies, we cannot compare them to the simulations for SON, which presented the opposite conditions from DJF. A more extensive study on the comparison between CMIP5 models and proxies with higher resolution is needed.

Finally, the model validation showed that there is still a need for improvements of the models, especially for better representing of the upper-level circulation during the austral spring and the amount of precipitation over northern South America and the Andean region. We believe our results provided a step further in the understanding of the dynamical mechanisms that are involved in the precipitation changes over South America during the Mid-Holocene.

Funding M.H. Shimizu would like to acknowledge FAPESP for the financial support through the PALaео-Constraints on Monsoon

Evolution and Dynamics (PACMEDY) project (No. 2016/24014-9) and Climate Research and Education in the Americas using Tree-ring and Speleothem Examples (PIRE-CREATE) project (No. 2017-50085-3).

References

- Adam O, Schneider T, Briant F (2018) Regional and seasonal variations of the double-ITCZ bias in CMIP5 models. *Clim Dyn* 51(1–2):101–117
- An SI, Choi J (2014) Mid-Holocene tropical Pacific climate state, annual cycle, and ENSO in PMIP2 and PMIP3. *Clim Dyn* 43:957–970
- Baker PA, Fritz SC (2015) Nature and causes of quaternary climate variation of tropical South America. *Quat Sci Rev* 124:31–47
- Baker PA, Rigsby CA, Seltzer GO, Fritz SC, Lowenstein TK, Bacher NP, Veliz C (2001a) Tropical climate changes at millennial and orbital timescales in the Bolivian Altiplano. *Nature* 409:698–701
- Baker PA, Seltzer GO, Fritz SC, Dunbar RB, Grove MJ, Tapia PM, Cross SL, Rowe HD, Broda JP (2001b) The history of South American tropical precipitation for the past 25,000 years. *Science* 291:640–643
- Barichivich J, Gloor E, Peylin P, Brienen RJ, Schöngart J, Espinoza JC, Pattanyak KC (2018) Recent intensification of Amazon flooding extremes driven by strengthened Walker circulation. *Science advances* 4(9):8785
- Berger A (1978) Long-term variations of caloric solar radiation resulting from the earth's orbital elements. *Quatern Res* 9:139–167
- Biasutti M, Battisti DS, Sarachik ES (2003) The annual cycle over the tropical Atlantic, South America, and Africa. *J Clim* 16:2491–2508
- Bird BW, Abbott MB, Rodbell DT, Vuille M (2011) Holocene tropical South American hydroclimate revealed from a decadal resolved lake sediment $\delta^{18}\text{O}$ record. *Earth Planet Sci Lett* 310(3–4):192–202
- Bothe O, Jungclaus JH, Zanchettin D (2013) Consistency of the multi-model CMIP5/PMIP3-past1000 ensemble. *Clim Past* 9:2471–2487
- Boullanger JP, Martinez F, Segura EC (2006) Projection of future climate change conditions using IPCC simulations, neural networks, and Bayesian statistics. Part 2: precipitation mean state and seasonal cycle in South America. *Clim Dyn* 28:255–271
- Braconnot P, Kageyama M (2015) Shortwave forcing and feedbacks in last glacial maximum and Mid-Holocene PMIP3 simulations. *Philos Trans R Soc A* 373(2054):20140424
- Braconnot P, Otto-Bliesner B, Harrison S, Joussaume S, Peterchmitt J-Y, Abe-Ouchi A, Crucifix M, Driesschaert E, Fichefet Th, Hewitt CD, Kageyama M, Kitoh A, Laine A, Loutre M-F, Marti O, Merkel U, Ramstein G, Valdes P, Weber SL, Yu Y, Zhao Y (2007a) Results of PMIP2 coupled simulations of the Mid-Holocene and last glacial maximum—part 1: experiments and large-scale features. *Clim Past* 3:261–277
- Braconnot P, Otto-Bliesner B, Harrison S, Joussaume S, Peterchmitt J-Y, Abe-Ouchi A, Crucifix M, Driesschaert E, Fichefet Th, Hewitt CD, Kageyama M, Kitoh A, Loutre M-F, Marti O, Merkel U, Ramstein G, Valdes P, Weber L, Yu Y, Zhao Y (2007b) Results of PMIP2 coupled simulations of the Mid-Holocene and last glacial maximum—Part 2: feedbacks with emphasis on the location of the ITCZ and mid- and high latitudes heat budget. *Clim Past* 3:279–296
- Braconnot P et al (2011) The paleoclimate modeling intercomparison project contribution to CMIP5. *CLIVAR Exchanges* 56(16):15–19
- Braconnot P, Harrison SP, Kageyama M et al (2012) Evaluation of climate models using palaeoclimatic data. *Nat Clim Change* 2:417–424

- Brady EC, Otto-Bliesner BL, Kay JE, Rosenbloom N (2013) Sensitivity to glacial forcing in the CCSM4. *J Clim* 26:1901–1925
- Carré M, Azzoug M, Bentaleb I, Chase BM, Fontugne M, Jackson D, Ledru M-P, Maldonado A, Sachs JP, Schauer AJ (2012) Mid-Holocene mean climate in the Southeastern Pacific and its influence on South America. *Quatern Int* 253:55–66
- Carvalho LMV, Jones C, Liebmann B (2002) Extreme precipitation events in Southeastern South America and large-scale convective patterns in the South Atlantic convergence zone. *J Clim* 15:2377–2394
- Cavalcanti I, Shimizu MH (2012) Climate fields over South America and variability of SACZ and PSA in HadGEM2-ES. *American Journal of Climate Change* 1:132–144
- Chan SC, Behera SK, Yamagata T (2008) Indian Ocean dipole influence on South American rainfall. *Geophys Res Lett* 35(14):L14S12. <https://doi.org/10.1029/2008GL034204>
- Chen TC, Weng SP, Schubert S (1999) Maintenance of austral summertime upper tropospheric circulation over tropical South America: the Bolivian high-nordeste low system. *J Climate* 18:320–330
- Cheng H, Sinha A, Cruz FW, Wang X, Edwards RL, d'Horta FM, Ribas CC, Vuille M, Stott LD, Auler AS (2013) Climate change patterns in Amazonia and biodiversity. *Nat Commun* 4:1411
- Cobb KM, Westphal N, Sayani HR, Watson JT, Di Lorenzo E, Cheng H, Edwards RL, Charles CD (2013) Highly variable El Niño—Southern oscillation throughout the Holocene. *Science* 339:67–70
- Coelho CAS, Cavalcanti IFA, Costa SMS, Freitas SR, Ito ER, Luz G, Santos AF, Nobre CA, Marengo JA, Pezza AB (2012) Climate diagnostics of three major drought events in the amazon and illustrations of their seasonal precipitation predictions. *Meteorol Appl* 19:237–255
- Collins WJ, Bellouin N, Doutriaux-Boucher M, Gedney N, Halloran P, Hinton T, Martin G (2011) Development and evaluation of an earth-system model-HadGEM2. *Geosci Model Dev* 4:1051
- Cook KH, Vizy EK (2006) South American climate during the last glacial maximum: delayed onset of the South American monsoon. *J Geophys Res* 111:D02110
- Cruz FWJ, Burns SJ, Karmann I, Sharp WD, Vuille M, Cardoso AO, Ferrari JA, Silva Dias PL, Viana OJ (2005) Insolation-driven changes in atmospheric circulation over the past 116,000 years in subtropical Brazil. *Nature* 434:63–66
- Cruz FW, Burns SJ, Karmann I, Sharp WD, Vuille M (2006) Reconstruction of regional atmospheric circulation features during the late pleistocene in subtropical Brazil from oxygen isotope composition of speleothems, earth planet. *Sci Lett* 248:495–507
- Cruz FW, Vuille M, Burns SJ, Wang X, Cheng H, Werner M, Edwards RL, Karmann I, Auler AS, Nguyen H (2009) Orbitally driven east-west anti-phasing of South American precipitation. *Nat Geosci* 2:210–214
- De Almeida RAF, Nobre P, Haarsma RJ, Campos EJD (2007) Negative ocean-atmosphere feedback in the South Atlantic convergence zone. *Geophys Res Lett* 34:L18809
- Dee DP et al (2011) The ERA-Interim reanalysis: configuration and performance of the data assimilation system. *Q J R Meteorol Soc* 137:553–597
- Dike VN, Shimizu MH, Diallo M, Lin Z, Nwofor OK, Chineke TC (2015) Modelling present and future African climate using CMIP5 scenarios in HadGEM2-ES. *Int J Climatol* 35:1784–1799
- Donohoe A, Marshall J, Ferreira D, McGee D (2013) The relationship between ITCZ location and cross-equatorial atmospheric heat transport; from the seasonal cycle to the last glacial maximum. *J Clim* 26:3597–3618
- Dufresne JL, Foujols MA, Denvil S et al (2013) Climate change projections using the IPSL-CM5 earth system model: from CMIP3 to CMIP5. *Clim Dyn* 40:2123–2165
- Espinoza JC, Ronchail J, Marengo JA, Segura H (2019) Contrasting North-South changes in Amazon wet-day and dry-day frequency and related atmospheric features (1981–2017). *Clim Dyn* 52(9–10):5413–5430
- Gan MA, Kousky VE, Ropelewski CF (2004) The South America monsoon circulation and its relationship to rainfall over West-Central Brazil. *J Climate* 17:47–66
- Garreaud RD, Vuille M, Compagnucci R, Marengo JA (2009) Present-day South American climate. *Palaeogeogr Palaeoclimatol Palaeoecol* 281:180–195
- Gent PR, Danabasoglu G, Donner LJ, Holland MM, Hunke EC, Jayne SR, Lawrence DM, Neale RB, Rasch PJ, Vertenstein M, Worley PH, Yang Z-L, Zhang M (2011) The community climate system model version 4. *J Clim* 24:4973–4991
- Giorgetta MA et al (2013) Climate and carbon cycle changes from 1850 to 2100 in MPI-ESM simulations for the coupled model intercomparison project phase 5. *J Adv Model Earth Syst* 5:572–597
- Harrison SP, Kutzbach JE, Liu Z, Bartlein PJ, Otto-Bliesner B, Muhs D, Prentice IC, Thompson RS (2003) Mid-Holocene climates of the Americas: a dynamical response to changed seasonality. *Clim Dyn* 20:663–688
- Haug GH, Hughen KA, Sigman DM, Peterson LC, Rohl U (2001) Southward migration of the intertropical convergence zone through the Holocene. *Science* 293:1304–1308
- Jones CD, Carvalho LMV (2013) Climate change in the South American monsoon system: present climate and CMIP5 simulations. *J Clim* 26:6257–6286
- Jones CD, Hughes JK, Bellouin N, Hardiman SC, Jones GS, Knight J, Liddicoat S, O'Connor FM, Andres RJ, Bell C, Boo K-O, Bozzo A, Butchart N, Cadule P, Corbin KD, Doutriaux-Boucher M, Friedlingstein P, Gornall J, Gray L, Halloran PR, Hurtt G, Ingram WJ, Lamarque J-F, Law RM, Meinshausen M, Osprey S, Palin EJ, Parsons Chini L, Raddatz T, Sanderson MG, Sellar AA, Schurer A, Valdes P, Wood N, Woodward S, Yoshioka M, Zerrouka M (2011) The HadGEM2-ES implementation of CMIP5 centennial simulations. *Geosci Model Dev* 4:543–570
- Kanner LC, Burns SJ, Cheng H, Edwards RL (2012) High-latitude forcing of the South American summer monsoon during the last glacial. *Science* 335,(6068):570–573. <https://doi.org/10.1126/science.1213397>
- Kanner LC, Burns SJ, Cheng H, Edwards RL, Vuille M (2013) High resolution variability of the South American summer monsoon over the last seven millennia: insights from a speleothem record from the central Peruvian Andes. *Quat Sci Rev* 75:1–10
- Kodama Y-M (1992) Large-scale common features of subtropical precipitation zones (the Baiu frontal zone, the SPCZ, and the SACZ), part I: characteristics of subtropical frontal zones. *J Meteorol Soc Jpn* 70:813–835
- Kodama Y-M (1993) Large-scale common features of sub-tropical convergence zones (the Baiu frontal zone, the SPCZ, and the SACZ), part II: conditions of the circulations for generating the STCZs. *J Meteorol Soc Jpn* 71:581–610
- Kousky VE (1988) Pentad outgoing longwave radiation climatology for the South American sector. *Rev Bras Meteor* 3:217–231
- Lenters JD, Cook KH (1997) On the origin of the bolivian high and related circulation features of the South American climate. *J Atmos Sci* 54:656–678
- Li G, Xie SP (2014) Tropical biases in CMIP5 multimodel ensemble: The excessive equatorial Pacific cold tongue and doubled ITCZ problems. *J Clim* 27(4):1765–1780
- Liu X, Battisti DS (2015) The influence of orbital forcing of tropical insolation on the climate and isotopic composition of precipitation in South America. *J Clim* 28:4841–4862
- Liu Z, Otto-Bliesner B, Kutzbach J, Li L, Shields C (2003) Coupled climate simulation of the evolution of global monsoons in the holocene. *J Clim* 16:2472–2490

- Liu Z, Harrison SP, Kutzbach J, Otto-Bliesner B (2004) Global monsoons in the Mid-Holocene and oceanic feedback. *Clim Dyn* 22:157–182
- Maksic J, Shimizu MH, Sampaio G, Venancio IM, Cardoso M, Ferreira FA (2019) Simulation of the holocene climate over South America and impacts on the vegetation. *Holocene* 29(2):287–299
- Marengo JA, Tomasella J, Alves LM, Soares WR, Rodriguez DA (2011) The drought of 2010 in the context of historical droughts in the Amazon region. *Geophys Res Lett* 38:L12703
- Marengo JA, Liebmann B, Grimm AM, Misra V, Silva Dias PL, Cavalcanti IFA, Saulo AC (2012) Recent developments on the South American monsoon system. *Int J Climatol* 32(1):1–21
- Marengo JA, Alves LM, Soares WR, Rodriguez DA, Camargo H, Riveros MP, Pabló AD (2013) Two contrasting severe seasonal extremes in tropical South America in 2012: flood in Amazonia and drought in northeast Brazil. *J Clim* 26(22):9137–9154
- McGee D, Donohoe A, Marshall J, Ferreira D (2014) Changes in the ITCZ location and cross-equatorial heat transport at the last glacial maximum, heinrich stadial 1, and the Mid-Holocene. *Earth Planet Sci Lett* 390:69–79
- Melo MLD, Marengo JA (2008) The influence of changes in orbital parameters over South American climate using the CPTEC AGCM: simulation of climate during the Mid-Holocene. *Holocene* 18:501–516
- Mohtadi M, Prange M, Steinke S (2016) Palaeoclimatic insights into forcing and response of monsoon rainfall. *Nature* 533:191–199
- Nobre P, Shukla J (1996) Variations of sea surface temperature, wind stress, and rainfall over the tropical Atlantic and South America. *J Clim* 9:2464–2479
- Novello V, Cruz F, Vuille M et al (2017) A high-resolution history of the South American monsoon from last glacial maximum to the holocene. *Sci Rep* 7:44267
- Prado LF, Wainer I, Chiessi CM (2013) Mid-Holocene PMIP3/CMIP5 model results: intercomparison for the South American monsoon system. *Holocene* 23(12):1915–1920
- Ramirez E, Hoffman G, Taupin JD, Francou B, Ribstein P, Caillon N, Ferron FA, Landais A, Petit JR, Pouyaud B, Schotterer U, Simoes JC, Stievenard M (2003) A new Andean deep ice core from Nevado Illimani (6350 m), Bolivia. *Earth Planet Sci Lett* 212:337–350
- Rotstayn LD, Jeffrey SJ, Collier MA, Dravitzki SM, Hirst AC, Syktus JJ, Wong KK (2012) Aerosol- and greenhouse gas-induced changes in summer rainfall and circulation in the Australasian region: a study using single-forcing climate simulations. *Atmos Chem Phys* 12:6377–6404
- Schmidt GA et al (2014) Configuration and assessment of the GISS ModelE2 contributions to the CMIP5 archive. *J Adv Model Earth Syst* 6:141–184
- Seltzer G, Rodbell D, Burns S (2000) Isotopic evidence for late quaternary climatic change in tropical South America. *Geology* 28:35–38
- Seth A, Rojas M, Rauscher SA (2010) CMIP3 projected changes in the annual cycle of the South American Monsoon. *Clim Change* 98:331–357
- Silva Dias PL, Turcq B, Silva Dias MAF, Braconnot P, Jorgetti T (2009) Mid-Holocene climate of tropical South America: a model-data approach. In: Vimeux F, Sylvestre F, Khodri M (eds) Past climate variability in South America and surrounding regions: from the Last Glacial Maximum to the Holocene. Springer, Dordrecht, pp 259–281. https://doi.org/10.1007/978-90-481-2672-9_11
- Strikis NM, Cruz FW, Cheng H, Karmann I, Lawrence Edwards R, Vuille M, Wang X, De Paula MS, Novello VF, Auler AS (2011) Abrupt variations in South American monsoon rainfall during the holocene based on a speleothems record from central-eastern Brazil. *Geology* 39:1075–1078
- Sueyoshi T et al (2013) Set-up of the PMIP3 paleoclimate experiments conducted using an earth system model, MIROC-ESM. *Geosci Model Dev* 6:819–836
- Taylor KE (2001) Summarizing multiple aspects of model performance in a single diagram. *J Geophys Res* 106:7183–7192
- Taylor KE, Stouffer RJ, Meehl GA (2012) An overview of CMIP5 and the experiment design. *Bull Am Meteorol Soc* 93:485–498
- Thompson LG, Mosley-Thompson E, Davis ME, Lin PN, Henderson KA, Cole-Dai J, Bolzan JF, Liu K (1995) Late Glacial stage and Holocene tropical ice core records from Huascaran, Peru. *Science* 269:46–50
- van Breukelen MR, Vonhof HB, Hellstrom JC, Wester WCG, Kroon D (2008) Fossil dripwater in stalagmites reveals Holocene temperature and rainfall variation in Amazonia. *Earth Planet Sci Lett* 275:54–60
- Vera C, Silvestri G (2009) Precipitation interannual variability in South America from the WCRP-CMIP3 multi-model dataset. *Clim Dyn* 32:1003–1014
- Vera C, Higgins W, Amador J, Ambrizzi T, Garreaud R, Gochis D, Gutzler D, Lettenmaier D, Marengo J, Mechoso CR, Nogues-Paegle J, Dias PL, Zhang C (2006) Toward a Unified View of the American Monsoon Systems. *J Clim* 19:4977–5000
- Virji H (1981) A preliminary study of summertime tropospheric circulation patterns over South America estimated from cloud winds. *Mon Weather Rev* 109:599–610
- Voltaire A, Sanchez-Gomez E, y Méliá DS, et al (2013) The CNRM-CM5.1 global climate model: description and basic evaluation. *Clim Dyn* 40:2091–2121
- Wang X, Edwards RL, Auler AS, Cheng H, Kong X, Wang Y, Cruz FW, Dorale JA, Chiang HW (2017) Hydroclimate changes across the Amazon lowlands over the past 45,000 years. *Nature* 541(7636):204
- Wang XY, Li X, Zhu J, Tanajura CA (2018) The strengthening of Amazonian precipitation during the wet season driven by tropical sea surface temperature forcing. *Environ Res Lett* 13(9):094015
- Watanabe S, Hajima T, Sudo K, Nagashima T, Takemura T et al (2011) MIROC-ESM 2010: model description and basic results of CMIP5-20c3m experiments. *Geosci Mod Dev* 4:845
- Xie P, Arkin PA (1997) Global precipitation: a 17-year monthly analysis based on gauge observations, satellite estimates, and numerical model outputs. *Bull Amer Meteor Soc* 78:2539–2558
- Xin X-G, Wu T-W, Zhang J (2013) Introduction of CMIP5 experiments carried out with the climate system models of Beijing climate center. *Adv Clim Change Res* 4:41–49
- Yin L, Fu R, Shevliakova E, Dickinson RE (2013) How well can CMIP5 simulate precipitation and its controlling processes over tropical South America? *Clim Dyn* 41:3127–3143
- Yoon JH, Zeng N (2010) An Atlantic influence on Amazon rainfall. *Clim Dyn* 34:249–264
- Yukimoto S et al (2012) A new global climate model of the meteorological research institute: MRI-CGCM3—model description and basic performance. *J Meteorol Soc Jpn* 90:23–64
- Zhang X, Liu H, Zhang M (2015) Double ITCZ in coupled ocean-atmosphere models: from CMIP3 to CMIP5. *Geophys Res Lett* 42(20):8651–8659

Publisher's Note Springer Nature remains neutral with regard to jurisdictional claims in published maps and institutional affiliations.